Hindawi
Wireless Communications and Mobile Computing
Volume 2024, Article ID 9428292, 15 pages
https://doi.org/10.1155/2024/9428292

Research Article

Analysis of Filtered Multicarrier Modulation Techniques Using Different Windows for 5G and Beyond Wireless Systems

Sourav Debnath, Samin Ahmed, and S. M. Shamsul Alam

Electronics and Communication Engineering Discipline, Khulna University, Khulna 9208, Bangladesh

Correspondence should be addressed to S. M. Shamsul Alam; alam_ece@yahoo.com

Received 7 May 2023; Revised 29 February 2024; Accepted 9 March 2024; Published 26 March 2024

Academic Editor: Ihsan Ali

In contemporary wireless communication systems, multicarrier modulation schemes have become widely adopted over single-carrier techniques due to their improved capacity to address challenges posed by multipath fading channels, leading to enhanced spectral efficiency. Orthogonal frequency division multiplexing (OFDM), a prevalent multicarrier scheme in 4G, is favored for its ease of implementation, interference resilience, and high data rate provision. But it falls short of meeting the requirements for 5G and beyond due to limitations such as out-of-band (OOB) emissions and cyclic prefixes. This paper introduces the filter bank multicarrier (FBMC) and universal filtered multicarrier (UFMC) with quadrature amplitude modulation (QAM) and phase shift keying (PSK) waveforms through Additive White Gaussian Noise channel (AWGN), Rayleigh fading channel and Rician channel. The objective of this paper is to enhance the performance of UFMC with reduced complexity through the new filtering approach for achieving optimal outcomes. The proposed scheme, incorporating Tukey filtering technique, demonstrates superior performance in reducing peak-to-average power ratio (PAPR) and improving bit error ratio (BER) compared to the original UFMC signal without necessitating additional power increments. Specifically, the UFMC system with Tukey filtering achieves a notable net gain of 5 dB. Simulation results demonstrate that utilizing various filter types in FBMC and UFMC systems, combined with QAM modulation, significantly reduces OOB emissions compared to conventional systems. In aspect to BER, Tukey window showed almost 10^{-6} at 15 dB SNR in UFMC which is better than FBMC.

1. Introduction

Wireless communication technology has revolutionized interpersonal interactions by seamlessly integrating mobility and communication. The insatiable need for gigabit-per-second (Gbps) data rates continues to rise, driven by new applications and users. The advent of 5G communication services represents a significant leap in coverage, quality of service (QoS), and applicability for various scenarios, including massive machine type communications (mMTC), internet of things (IoT), and ultrareliable, low-latency communications (uRLLC). 5G stands out with its tenfold increase in data rates compared to 4G, enabling innovative use cases. 5G's ultrareliable and low-latency features are vital for mission-critical applications like autonomous vehicles, remote surgery, and industrial automation. In essence, 5G serves as a comprehensive technological solution, leveraging preexisting technologies to address diverse communication scenarios. Within this framework, multicarrier modulation (MCM) emerges as a key technique, dividing data into multiple components and transmitting them as separate carrier signals. Despite the historical success of orthogonal frequency division multiplexing (OFDM) in mitigating multipath fading, it faces challenges in the 5G landscape. The transition to 5G, with technologies like millimeter-wave communication and massive multiple-input multiple-output (MIMO) systems, presents unique challenges for OFDM. As 5G continues to expand its capabilities, alternative modulation technologies may be explored to overcome the shortcomings of OFDM in meeting the diverse and demanding requirements of emerging applications in wireless communication. These challenges include increased susceptibility to frequency-selective fading, inefficient use of spectral resources, and limited support for advanced beam forming techniques. Consequently, 5G has spurred the development of alternative modulation and waveform schemes, such as filtered OFDM (f-OFDM), universal filtered multicarrier

(UFMC), and generalized frequency division multiplexing (GFDM). These approaches aim to address the evolving needs of 5G communications by providing improved spectral efficiency, enhanced robustness in diverse channel conditions, and support for advanced antenna technologies [1]. Successfully supporting many types of services with high data rates, huge bandwidth, multiple access, low bit error ratio (BER), and high throughput must be considered. Under these situations, OFDM in 4G technologies is incapable of meeting a broad range of services in a variety of scenarios. However, the discontinuous spectrum of carrier aggregation is limited by increased frequency offset, out-of-band (OOB) emission, and time synchronization limit. Time synchronization is a major concern of the physical layer for wireless communication [2]. To meet those versatile requirements, different MCM approaches, such as filter bank multicarrier (FBMC), and UFMC are now in the research process for 5G.

In recent times, several alternative technologies have emerged as candidates for the 5G air interface, diverging from the traditional OFDM approach. Among these innovations are f-OFDM, FBMC, UFMC, and GFDM. Each of these approaches exhibits distinct advantages and tradeoffs. In the FBMC modulation scheme, a notable departure from conventional OFDM is observed, as it employs individual filtering for each subcarrier via a filter bank. This meticulous filtering process significantly mitigates OOB emissions, consequently reducing intercarrier interference (ICI). However, it is imperative to acknowledge that FBMC's superiority in spectral containment necessitates a more complex hardware infrastructure due to the required filter length. In contrast, the UFMC system adopts a different strategy by aggregating and filtering subcarriers into sub-bands [3]. Additionally, UFMC boasts several merits, including reduced side lobe radiation, low latency, support for frequency segmentation, and multiservice applications. Its adaptability to short burst communications further enhances its appeal. UFMC's utilization of Dolph–Chebyshev (DC) filters for each sub-band merits attention, as it allows valuable signals to pass through the pass band without any loss while rapidly decaying frequency response in the stop band helps curtail OOB emissions. Notably, UFMC retains fundamental characteristics of OFDM, rendering it pertinent to MIMO applications. This adaptability to MIMO systems further underscores the versatility and potential of UFMC within the evolving landscape of wireless communications.

Numerous efforts have been made to address the task of enhancing performance when dealing with UFMC systems. The primary focus of this research paper is to identify the most promising candidate for 5G technology through a comprehensive analysis and comparison of various modulation schemes, including quadrature amplitude modulation (QAM) and phase shift keying (PSK), as well as modifying the conventional window filtering techniques by applying different filtering methods such as Hamming, Hanning, Blackman, Kaiser, and Tukey window applied to FBMC and UFMC systems. The study involves an extensive evaluation of key performance metrics, including peak-to-average power ratio (PAPR) and BER, under different channel conditions, specifically Additive White Gaussian Noise (AWGN) and Rayleigh fading channels. Additionally, the paper conducts a comparative analysis between the utilization of PHYDYAS and Chebyshev filters within the UFMC framework, with a specific focus on their impact on BER and PAPR. To ensure the practical relevance and validity of the simulated BER results, a comprehensive theoretical BER model has been developed and presented alongside the simulation outcomes. Also, Complementary Cumulative Distribution Function (CCDF) is simulated to verifying the calculation proposed system PAPR. This rigorous approach not only provides valuable insights into the performance of FBMC and UFMC systems but also contributes to the selection of the most suitable and less complex technology for 5G applications.

2. Literature Review

A lot of work has been done on FBMC and UFMC. We selected some latest papers and tried to find out our paper's uniqueness. Summarization of some recent papers are described below:

The research introduced novel pulse shaping filters for FBMC/OQAM systems and evaluated their characteristics. They compared FBMC/OQAM performance in various channels based on power spectral density (PSD), spectral efficiency (SE), signal-to-interference ratio (SIR), carrier frequency offset (CFO), and BER. Furthermore, the authors suggested a FBMC/OQAM strategy using frequency/time block spreading through Walsh–Hadamard codes [4].

The authors conducted a comprehensive analysis of the UFMC system, focusing on several key performance metrics including SE, BER, PAPR, CFO, and the impact of various multipath fading channels and timing delays (TD). They developed a rigorous mathematical model to precisely calculate the BER for the UFMC system, providing a closed-form equation for this critical parameter. Additionally, the authors derived an equivalent representation of the transmitter in the frequency domain. Furthermore, they presented the outcomes of Monte Carlo simulations specifically related to UFMC, offering valuable insights into the system's performance under various conditions. This research provides a substantial contribution to the understanding and evaluation of UFMC system performance, offering a solid foundation for further study and practical applications [1].

Farhang-Boroujeny [5] pointed out the drawbacks of OFDM related to the "subset of subcarriers" issue in their research and endorsed the FBMC system as a superior alternative [5].

Kim et al. [6] introduced QAM–FBMC, a novel waveform that improves spectrum confinement and efficiency compared to cyclic prefix-OFDM (CP-OFDM). Their study on QAM–FBMC transmission and reception techniques demonstrated higher spectrum efficiency compared to CP-OFDM [6].

A comparative analysis of various FBMC used pulse shaping filters, such as rectangle, extended rectangular, RRC (root raised cosine), optimum finite duration pulse, Hermite, PHYDYAS, and IOTA filters. Notably, instead of using CP in FBMC, Hermite and IOTA filters showed better SIR in high-frequency

dispersion scenarios and lower sidelobe levels. PHYDYAS filters, on the other hand, demonstrated the best SIR performance, offering simplified receiver and transmitter design possibilities [7].

Sakkas et al. [8] conducted a comprehensive investigation into the UFMC system, specifically focusing on its design aspects with regard to BER performance in relation to sub band filter length. This paper explored the enhancement of UFMC performance in parallel processing environments by investigating the impact of employing large FFT and M-QAM values. The increased computational complexity associated with larger FFT and M-QAM values can be mitigated through multiprocessing techniques, resulting in overall performance improvement [8].

In their study on 5G communications, Baki et al. [9] introduced two distinct prototype filters for FBMC and UFMC systems. Specifically, they proposed the utilization of a Binomial Filter for FBMC and a Fractional Powered Binomial Filter (FPBF) for UFMC. Comparative analysis revealed that the Binomial Filter in FBMC significantly reduces PAPR by approximately 0.81 dB at the 256-QAM level, when compared to another widely used Prototype Filter. Additionally, in the case of UFMC with the FPBF, the sub-band interference is notably 58 dB lower than that of UFMC using a 60 dB DC Filter. Furthermore, the PAPR is minimized in the context of FPBF-based UFMC [9].

Guo et al. [10] focused their research on minimizing the computational complexity of UFMC technology. They achieved this by introducing two key structural enhancements: the FIR (finite impulse response) filter structure and the polyphase filter structure, both implemented through a lightweight approach. These modifications were integrated into the UFMC transmitter design with the dual aim of reducing computational demands and maintaining signal accuracy. As a result of their efforts, the UFMC transmitter's computational complexity was significantly reduced, showcasing the potential of these techniques to enhance the efficiency of UFMC technology [10].

Hussain and Audah [11] introduced a novel approach in the context of UFMC communication, integrating BCH (Bose–Chaudhuri–Hocquenghem) codes within the system. Their research focused on employing BCH codes over an AWGN channel within the UFMC framework. Their findings indicated that the integration of BCH codes in UFMC resulted in improved BER performance. Additionally, their approach demonstrated a more effective reduction in both PAPR and OOBE values compared to conventional OFDM systems [11].

In order to mitigate spectral leakage issues within adjacent sub-bands, a novel approach has been proposed involving the utilization of Kaiser–Bessel filter-based pulse shaping, as opposed to the conventional DC filter, for UFMC-based waveforms. This strategy has been further examined through a comprehensive analysis, encompassing PSD, CCDF, and adjacent channel power ratio (ACPR) assessments. The simulation results revealed that UFMC (Kaiser-based window) exhibits superior power spectral density and reduced sidebands in comparison to UFMC (Dolph–Chebyshev) and conventional OFDM. Specifically, UFMC with Kaiser–Bessel windowing demonstrated a higher power spectral density and exhibits reduced sideband interference. This signifies its potential for enhancing spectral efficiency and minimizing interference in communication systems, thereby presenting a promising alternative in waveform design for future applications [12].

Dhua et al. [13] conducted an analysis of FBMC-based wireless systems with fewer subcarriers, demonstrating superior performance in latency and BER compared to f-OFDM systems, while also boasting lower computational complexity. It's worth noting that for higher order modulations, FBMC's BER performance declines due to increasing interference levels [13].

A study conducted by Molla et al. [14] suggests that UFMC exhibits promise as a next-generation modulation scheme when compared to OFDM. This conclusion is drawn from their investigation of simulated PSD and BER performance across varying numbers of subcarriers and filter length values [14].

Ramavath et al. [15] introduced a CP-based FBMC system, which involves the addition of a cyclic prefix to the transmitted signal. This technique effectively reduces the impact of multipath fading and intersymbol interference (ISI). Notably, CP-based FBMC systems exhibit superior performance in terms of PSD compared to traditional FBMC systems [15].

3. Mathematical Analysis

This section systematically describes transceiver systems of OFDM, FBMC, and UFMC in term of mathematics equations. After that the theoretical for PAPR, PSD, BER are described. Then, AWGN and Rayleigh Fading channels basic equations are explained. Finally, the mathematical equations of different window filtering techniques that are applied to FBMC and UFMC are described respectively, which are reliable and valid.

3.1. Orthogonal Frequency Division Multiplexing (OFDM). OFDM, is a twin-frequency division multiplexing system, akin to FDM principles [16]. In OFDM, diverse information carriers are employed to transmit data. Prior to transmission, these signals in the frequency domain are transformed into the time domain through the use of the IFFT technique. IFFT adjusts the length of complex data points to a power-of-two configuration in the time domain, facilitating efficient transmission [17].

Transmitted data is subdivided into subcarriers with a CP for ISI mitigation, replacing filters and oscillators. At the receiver, FFT transforms the time domain signal into the frequency domain, as depicted in Figure 1.

3.2. Properties of Orthogonality in OFDM. Orthogonality is an important key element in OFDM because the lack of guard bands between the subcarriers. Because all of the subcarriers are close together, their spectra overlap each other. On the other hand, each subcarrier frequency corresponds with zero power in all other subcarriers, the expected mutual interference does not occur.

Let us consider complex signals $\{e^{j2\pi f_k t}\}_{k=0}^{N-1}$ in OFDM which is time limited and represents different subcarriers

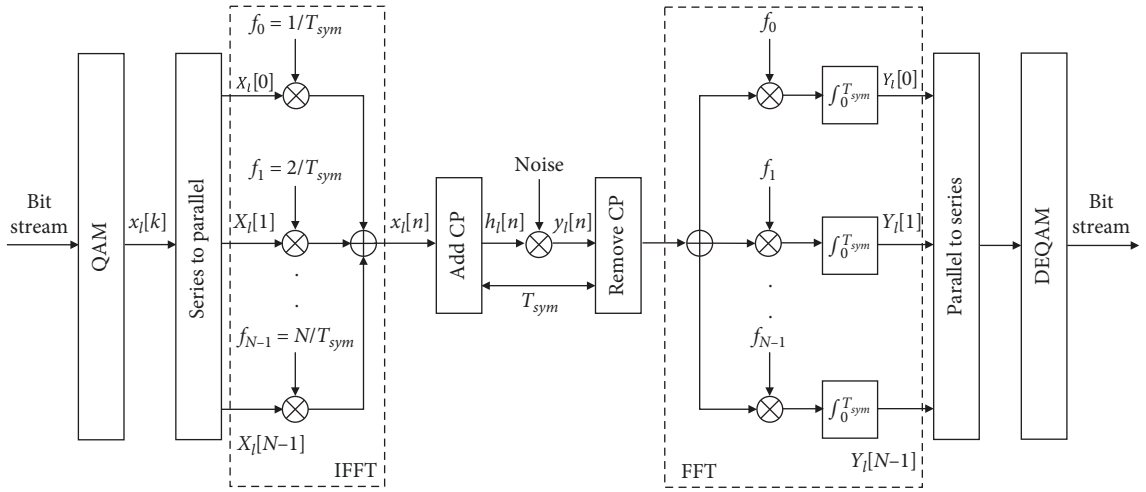

FIGURE 1: Visualize transceiver diagram of OFDM [18].

at $f_k = k/T_{\text{sym}}$, where $0 \le t \le T_{\text{sym}}$. It will be orthogonal if the integral of the fundamental period product is zero. In Equation 1, the orthogonality can be expressed as [18].

$$\frac{1}{T_{\text{sym}}}\int_0^{T_{\text{sym}}} e^{j2\pi f_k t} e^{-j2\pi f_i t}\,dt = \frac{1}{T_{\text{sym}}}\int_0^{T_{\text{sym}}} e^{j2\pi \frac{k-i}{T_{\text{sym}}} t}\,dt. \tag{1}$$

At $t = nT_s = nT_{\text{sym}}/N, n = 0, 1, 2, \ldots\ldots, N-1$, the above signal in discrete time domain can be written in Equation 2 as [18].

$$\begin{aligned}\frac{1}{N}\sum_{n=0}^{N-1} e^{j2\pi \frac{k}{T_{\text{sym}}} nT_s} e^{-j2\pi \frac{i}{T} nT_s} &= \frac{1}{N}\sum_{n=0}^{N-1} e^{j2\pi \frac{k}{T_{\text{sym}}} \frac{nT}{N}} e^{-j2\pi \frac{i}{T_{\text{sym}}} \frac{nT_{\text{sym}}}{N}} \\ &= \frac{1}{N}\sum_{n=0}^{N-1} e^{j2\pi \frac{(k-i)}{N} n} = \begin{cases} 1, \forall \text{integer} k = i \\ 0, \text{Otherwise} \end{cases}.\end{aligned} \tag{2}$$

3.3. Transmitter Block in OFDM. The OFDM transmitter maps the message bits into a sequence of PSK or QAM symbols, which are later converted into N parallel streams. In OFDM, several complex-valued subcarriers are modulated in each symbol period. Let the message signal, $X_l[k]$ denote the l^{th} transmit symbol at the k^{th} subcarrier, where $l = 0, 1, 2\ldots.$, and $k = 0, 1, 2\ldots\ldots, N-1$. N denotes the total number of subcarriers. The l^{th} OFDM signal at the k^{th} subcarrier can be expressed in Equation 3 as [18].

$$\Psi_{l,k}(t) = \begin{cases} e^{j2\pi f_k \left(t - lT_{\text{sym}}\right),} & < t < T_{\text{sym}} \\ 0 & \text{elsewhere} \end{cases}. \tag{3}$$

In the continuous-time domain, the passband and baseband OFDM signals can be represented in Equations 4 and 5, respectively [18].

$$x_l(t) = \text{Re}\left\{\frac{1}{T_{\text{sym}}}\sum_{l=0}^{\infty}\left\{\sum_{k=0}^{N-1} X_l[k]\Psi_{l,k}(t)\right\}\right\}, \tag{4}$$

and

$$x_l(t) = \sum_{l=0}^{\infty}\sum_{k=0}^{N-1} X_l[k] e^{j2\pi f_k \left(t - lT_{\text{sym}}\right)}. \tag{5}$$

The complex time domain sequence is then generated using IDFT and a CP, and it is sent over the channel. The continuous-time baseband signal at $t = lT_{\text{sym}} + nT_s$ with $T_s = T_{\text{sym}}/N$ and $f_k = k/T_{\text{sym}}$ to obtain the discrete time OFDM symbol. Thus, the following equation can be found in Equation 6 [18].

$$x_l[n] = \sum_{k=0}^{N-1} X_l[k] e^{\frac{2\pi kn}{N}} \text{for } n = 0, 1, \ldots, (N-1), \tag{6}$$

where $X_l[k]$ is complex symbol transmitted over the k^{th} subcarrier. The above equation is the N-point IDFT of PSK or QAM data symbols $\{X_l[k]\}_{k=0}^{N-1}$, which can be quickly calculated with the IFFT technique. After that CP was added with the actual OFDM signal.

3.4. Insertion of Cyclic Prefix with OFDM Transmitted Signal. There are two ways to insert guard interval in OFDM. One is zero padding (ZP) and another is CP. In this research study, CP is used instead of ZP. The cyclic extension of an OFDM symbol is referred to as the CP. It acts as a guard interval in OFDM, preventing ISI from the preceding symbol.

Let the CP length of each sample is T_{G}. So, the symbol duration of extended OFDM is $T_{\text{sym}} = T_{\text{sub}} + T_{\text{G}}$.The CP has guaranteed the continuity of each delayed subcarrier, and its orthogonality with all other subcarriers is sustained over T_{sub} in Equation 7 [18].

$$\frac{1}{T_{\text{sub}}}\int_0^{T_{\text{sub}}} e^{j2\pi f_k(t-t_0)}e^{-j2\pi f_i t-t_0)}dt = 0, k \neq i. \tag{7}$$

In Equation 8, arrival of the first OFDM signal with a delay of t_0. So,

$$\frac{1}{T_{\text{sub}}}\int_0^{T_{\text{sub}}} e^{j2\pi f_k(t-t_0)}e^{-j2\pi f_i t-t_0-T_s)}dt = 0, k \neq i. \tag{8}$$

3.5. Receiver Block of OFDM. At the receiving end, the transmitted signals are received which is passed over the channel. The received signal in discrete frequency domain $y_l[n]$ can be represented as $y_l[n] = h[m] \times x[n-m] + z_l[n]$, where $h[m] =$ Channel impulse in discrete time domain and $z_l[n] =$ AWGN noise in discrete time domain. Then removing CP and using DFT, the actual OFDM signal is converted to frequency domain from time domain and will be extracted. In frequency domain, the signal can be expressed in Equation (9) as [18].

$$\begin{aligned} Y_l[k] &= \sum_{n=0}^{N-1} y_l[n]e^{-j2\pi kn/N} = \sum_{n=0}^{N-1}\left\{\sum_{m=0}^{\infty} h_l[m]x_l[n-m] + z_l[n]\right\}e^{-j2\pi kn/N} \\ &= \sum_{n=0}^{N-1}\left\{\sum_{m=0}^{\infty} h_l[m]\left\{\frac{1}{N}\sum_{i=0}^{N-1} X_l[i]e^{j2\pi i(n-m)/N}\right\}\right\}e^{-j2\pi kn/N} + Z_l[k] \\ &= \frac{1}{N}\sum_{i=0}^{N-1}\left\{\underbrace{\left\{\sum_{m=0}^{\infty} h_l[m]e^{-j2\pi im/N}\right\}}_{\text{Channel Frequency Response}} \underbrace{X_l[i]\sum_{n=0}^{\infty} e^{-j2\pi(k-i)n/N}}_{\text{Transmitted signal in frequency domain}}\right\}e^{-j2\pi kn/N} + \underbrace{Z_l[k]}_{\text{AWGN Noise}} \end{aligned} \tag{9}$$

3.6. Filter Bank Multicarrier (FBMC). One of the most significant disadvantages of OFDM is the poor spectral behavior induced by the usage of CP, which FBMC overcomes by including a generalized pulse shaping prototype filter and providing well-localized subchannels in both the time and frequency domains. FBMC systems have received much attention as an alternative to traditional OFDM systems. FBMC has an asynchronous transfer function and tunable parameters. Only the adjacent subchannels must be orthogonal in FBMC. FBMCs are classified into three types: multitone faltering FBMC (FMT/FBMC), multitone cosine modulated FBMC (CMT/FBMC), and offset quadrature amplitude modulated FBMC (OQAM/FBMC) [17]. Mainly, OQAM-FBMC is being focused. This is based on QAM symbols with in-phase and quadrature components that are half the symbol period apart. It is feasible to employ OQAM modulation to utilize the entire channel bandwidth. Instead of CP, filter techniques are applied in FBMC.

The prototype filter is a zero-frequency carrier filter and serves as the basis for other subcarrier filters [19]. The number of overlapping multicarrier symbols in the time domain is known as the overlapping coefficient, characterizing the filter. Using prototype filters, the FBMC system has lower spectral sidelobes compared to traditional OFDM systems. A filter bank, namely synthesis filter bank, is used at the transmitting end, whereas a filter bank, namely analysis filter bank, is used at the receiving end. Figure 2 describes the visualize transceiver system of FBMC.

3.7. Transmitter Block in FBMC. From Figure 2, the information bits are sent through QAM mapping at the transmitter, and the k^{th} subcarrier of the l^{th} time, $a_k(l)$ is generated. OQAM preprocessing is necessary to obtain an OQAM signal. Using complex-to-real conversion (C2R), the complex signal $a_k(l)$ is transformed to a real signal and divided into two new signals, $d_k(n)$ and $d_k(n+1)$. Even and odd numbered subchannels have separate complex to real transforms, which may be expressed in Equations (10) and (11) respectively as [21].

$$d_k(n) = \begin{cases} \text{Re}(a_k(l)), k = \text{even}, \\ \text{Imag}(a_k(l)), k = \text{odd}, \end{cases} \tag{10}$$

$$d_k(n+1) = \begin{cases} \text{Imag}(a_k(l)), k = \text{even}, \\ \text{Re}(a_k(l)), k = \text{odd}, \end{cases} \tag{11}$$

where Re(.) and Imag(.) are the real and the imaginary part of the signal, respectively. For obtaining symbol orthogonality, $d_k(n)$ signal is multiplied by $\theta_k(n) = j^{k+n}$. OQAM signal, $x_k(n)$ is expressed in Equation (12) [21].

$$s[m] = \sum_{k=0}^{M-1}\sum_{-\infty}^{\infty} x_k(n)\underbrace{h_k\left(m - n\frac{M}{2}\right)e^{\frac{j2\pi}{M}\text{km}}}_{\textbf{Filter response}}, \tag{12}$$

where $s[m] =$ Transmitted signal in discrete time domain, $M =$ number of subchannels.

3.8. PHYDYAS Prototype Filter. The designed prototype filter is a PHYDYAS filter bank which is symmetrical. As frequency sampling technique is used in prototype filter, the design structure of frequency sampling technique is very simple. The goal is to directly project the optimal sampling point in the frequency domain using a frequency domain filter response expression, and then apply the IFT to obtain the filter values

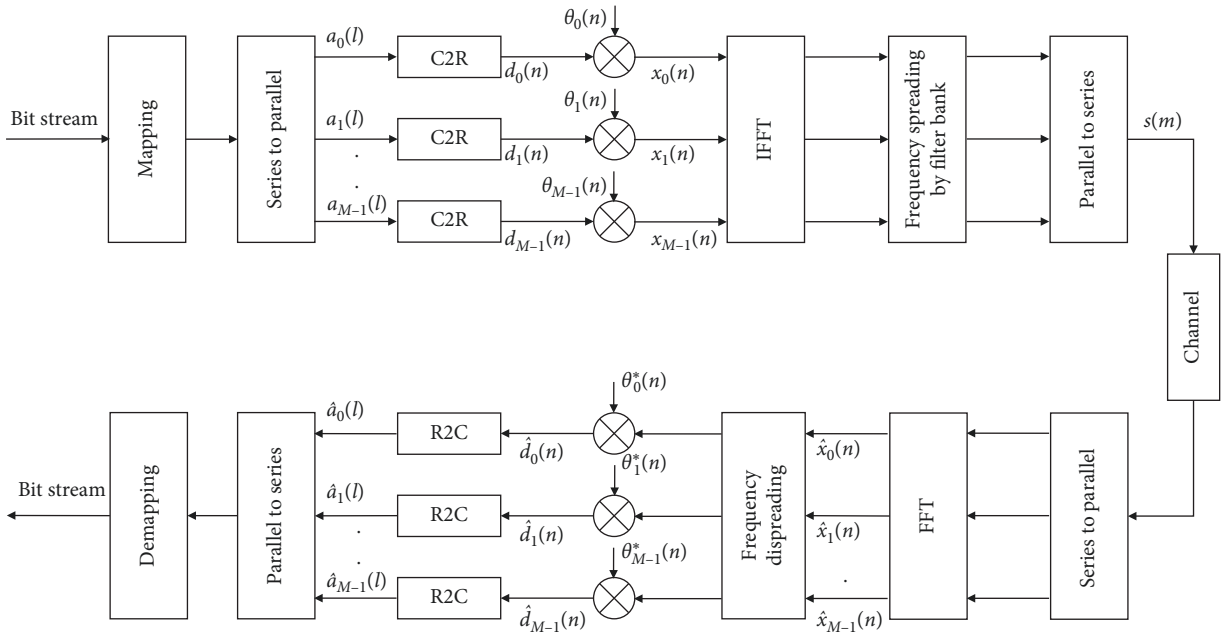

FIGURE 2: Visualize transceiver diagram of FBMC [20].

in the time domain. The frequency response of the filter can be written as [22].

$$H(f) = \sum_{k=-(K-1)}^{K-1} H_k{}^2 \frac{\sin\left(\pi\left(f - \frac{k}{\mathrm{MK}}\right)\mathrm{MK}\right)}{\mathrm{MK}\sin\left(\pi\left(f - \frac{k}{\mathrm{MK}}\right)\right)}, \tag{13}$$

where $K =$ overlapping factor.

3.9. Receiver Block in FBMC. The transmitted signal $s[m]$ is passed over the AWGN channel and affected by some noise. At the receiving end, the demodulated signal $Y[k]$ can be obtained by the projection of the received signal $r[m]$ in discrete time domain is expressed in Equation (14) [4].

$$Y[k] = \sum_{k=-\infty}^{+\infty} r[m]\widehat{h}_k[m - nM/2] + Z[K], \tag{14}$$

where $\widehat{h}_k[m] = h_k^*[m] = e^{-j\frac{2\pi}{M}\mathrm{km}}h[k]$ and $Z[K] =$ AWGN in frequency domain.

3.10. Universal Filtered Multicarrier (UFMC). UFMC is a noble multicarrier modulation technique that combines the advantages of OFDM and filter bank in FBMC. Instead of filtering the entire signal at once in OFDM or filtering each subcarrier in FBMC, the group of subcarriers is filtered in UFMC.

From Figure 3, it can be seen that, in UFMC transmission, first the total bandwidth is divided into several sub-bands and each sub-band consists of a certain number of subcarriers. By using the series-to-parallel converter, the data bits are then converted in parallel. The time-domain of the signal is changed to the frequency domain by the N-point IFFT [24]. In this case, the IFFT operator acts as a modulator, which ensures that the sub-band carriers do not interfere with one another [25]. The output of the IFFT is serialized by parallel to the serial converter and then filtered with the necessary filter. After that, each filter output is assembled, and the final signal is sent through the channel. The received data from the channel is passed through the series to parallel converter. Zero padding is required for adding the guard interval of zeros. This eliminates ISI caused by Transmitter filter delay. Furthermore, $2N$ point FFT converts the received data from the frequency domain to the time domain. Lastly, the symbol demapping process is used to convert the data symbols into bits and retrieve the original data.

3.11. Transmitter Block of UFMC. In UFMC, the subcarrier group is filtered. Let, for the k^{th} user, total number of sub bands is B_k, total number of subcarriers is N_k and each sub band consists of M-users. Consider in the i^{th} sub-band there are N_i subcarriers. So, $\sum_{i=1}^{B_k} N_i = N_k$. N_i complex symbols sequence is transformed into a block of N_i parallel symbols. By N-point IFFT, N_i length of each sub-band frequency domain signal $S_i(k)$ will be converted into discrete time domain signal which shown in Equation (15) [23].

$$s_i(l) = \frac{1}{\sqrt{N}} \sum_{k=O_i} S_i(k) e^{j2\pi kl/N}, l = 0, 1, \ldots.., N-1, \tag{15}$$

where $O_i =$ subcarrier indices in the sub-band i. After that filtering is applied on each sub-band sequence which is represented as $s_i(l)$, passed through a corresponding impulse response of FIR filter, $f_i(l)$ of L length to reduce OOB leakage. Filter is modulated to the proper frequency by multiplying a prototype impulse response $f(l)$ with an exponential sequence, that is $f_i(l) = f(l)e^{j\pi l(M-1)/N}$. In this theoretical expression, DC window with adjustable sidelobe attenuation is considered. After FIR filtering, the transmitted signal in discrete time domain for i^{th} sub-band is shown in Equation (16) [23].

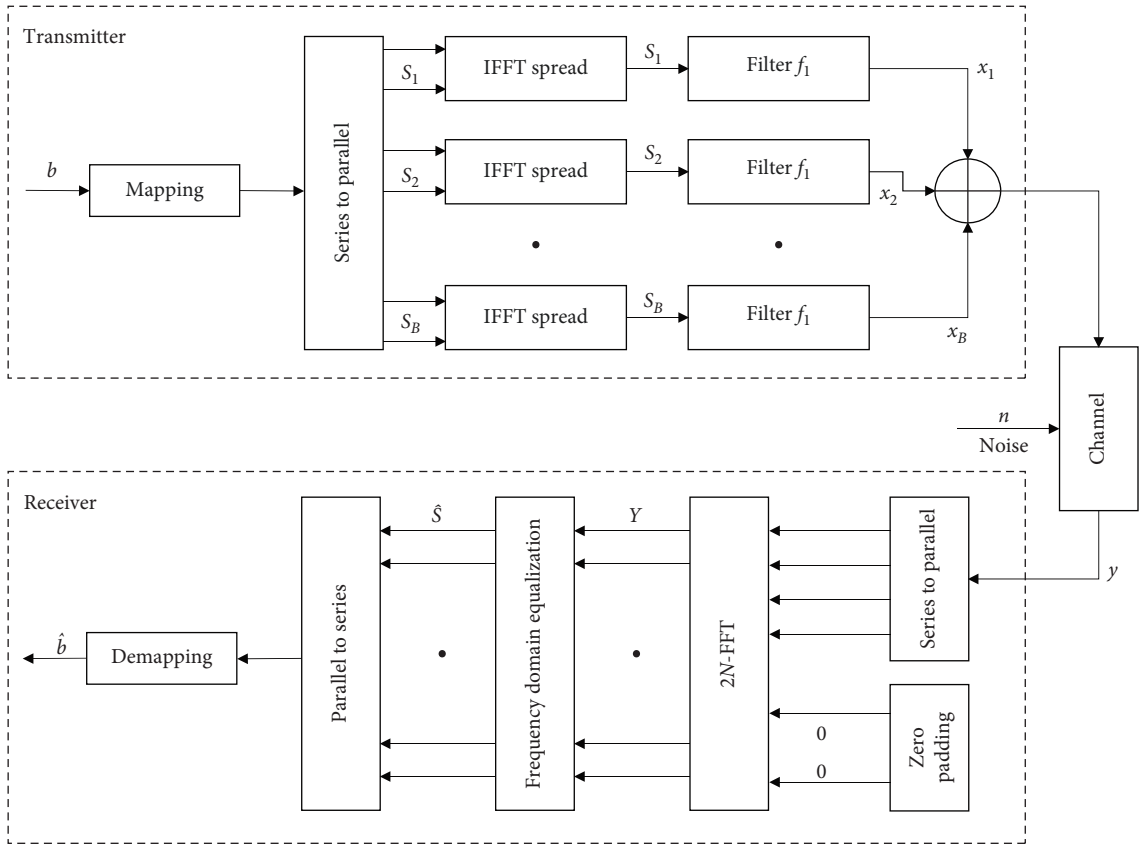

FIGURE 3: Visualize transceiver diagram of UFMC [23].

$$x_i(l) = s_i(l) * f_i(l) \text{where index}, l = 0, 1, \ldots, N + L - 2, \tag{16}$$

where $*$ indicates the discrete time convolution. The summation of different sub-band signals is written in Equation (17).

$$x(l) = \sum_{i=1}^{B} x_i(l) \tag{17}$$

By putting Equations (15) and (16) in Equation (17) we get,

$$x(l) = \frac{1}{\sqrt{N}} \sum_{n=0}^{N-1} \sum_{k=0}^{N-1} S(k) e^{\frac{j2\pi kl}{N}} f(l-n) \tag{18}$$

Finally, discrete time signal, $x(l)$ found in Equation 18 is ready for transmission.

3.12. Dolph–Chebyshev (DC) Filtering Approach in UFMC. Several filters have been existed but the classical UFMC system is used DC filter technique. It is used to reduce the OOB spectral emissions. The DC window is defended in the frequency domain by the following Equation 19.

$$F(\omega) = \frac{C_{L-1}\left(x_0 \cos\left(\frac{\omega}{2}\right)\right)}{C_{L-1}(x_0)}, \tag{19}$$

where x_o = adjustable parameter and $C_m(x) = m^{\text{th}}$ order Chebyshev polynomials. At sampled frequencies $\omega_k = 2\pi k/L$, the L^{th} order DC window in the frequency domain can be expressed as in Equation 20 [26].

$$F(\omega) = \frac{C_{L-1}(x_0 \cos(\pi K/L))}{C_{L-1}(x_0)}, \tag{20}$$

where L(even) represents filter order and index $k = (-\frac{L}{2} - 1), \ldots\ldots\ldots, -1, 0, 1$. Following this, the coefficients of the discrete-time DC filter's impulse response $f(l)$ is obtained by taking the IDFT of F_k and scaling the result to have a peak value of one. This can be formulated in Equation 21 as:

$$f(l) = \sum_{k=-\left(\frac{L}{2}-1\right)}^{\left(\frac{L}{2}-1\right)} F_k e^{\frac{2\pi jkl}{L}} \tag{21}$$

Due to the symmetry in $F(\omega)$, we assume that the window $f(l)$ has real-valued coefficients. Consequently, in Equation 22, we can also write $f(l)$ as:

$$f(l) = \frac{1}{L}\left\{1 + 2r\sum_{k=1}^{\frac{L-1}{2}}\left(x_0\cos\left(\frac{\pi k}{L}\right)\right)\left(\cos\left(\frac{2\pi kl}{L}\right)\right)\right\}, \tag{22}$$

where $x_0 = \cosh(\frac{1}{L-1}\cosh^{-1}(\frac{1}{r}))$and r is defined as the stopband ripple [26].

3.13. Receiver Block of UFMC. With $2N$-point FFT and ZP operations, the received signal in frequency domain is represented in Equation 23 [23].

$$Y(m) = \frac{1}{\sqrt{2N}}\left\{h(k)\sum_{l=n}^{L+n-1}\sum_{n=0}^{N-1}\sum_{k=0}^{N-1}S(k)\underbrace{f(l-n)e^{-j2\pi\left(\frac{ml}{2}-kn\right)/N}}_{\text{Filter Response}}\right\} + Z(k) \tag{23}$$

For even subcarriers ($m = 0, 2, \ldots, 2N-2$), k in frequency domain is divided into two stages written in Equations 24 and 25, *r*espectively. When $k = \frac{m}{2}$, then

$$Y(m) = \frac{1}{\sqrt{2N}}\left\{H\left(\frac{m}{2}\right)\sum_{l=n}^{L+n-1}\sum_{n=0}^{N-1}S\left(\frac{m}{2}\right)f(l-n)e^{-j2\pi\frac{m}{2}(l-n)/N}\right\} + Z\left(\frac{m}{2}\right), \tag{24}$$

when $k \neq \frac{m}{2}$

$$Y(m) = \frac{1}{\sqrt{2N}}\left\{H(k)S(k)\sum_{l=0}^{L-1}f(l)e^{\frac{-j2\pi\frac{m}{2}l}{N}}\sum_{n=0}^{N-1}e^{-j2\pi\left(\frac{m}{2}l-k\right)n/N}\right\} + Z(k). \tag{25}$$

3.14. Analysis of Peak to Average Power Ratio (PAPR). PAPR is described the envelope fluctuation of multicarrier modulation schemes. PAPR occurs after an IFFT procedure, in which data symbols from many sources are added together to give a high peak value. The PAPR of multicarrier modulation techniques can be defined in Equation (26) as [18].

$$\text{PAPR} = \frac{P_{\text{peak}}}{P_{\text{average}}} = \frac{\max_{n=0,1,2,\ldots\ldots N-1}|x(t)|^2}{E|x(t)|^2}, \tag{26}$$

where E = Expected value, P_{peak} = Peak power of transmitted signal, and P_{average} = Average power of transmitted signal.

The CCDF of signals for the proposed UFMC system can be defined as:

$$P(\text{PAPR} > \text{PAPR}_o) = 1 - (1 - e^{-\text{PAPR}_o})^N, \tag{27}$$

where PAPR_o = The clipping level.

3.15. Window Mapping by Discrete Fourier Transform (DFT). Window functions are used to restrict a signal in time (to make it shorter) or to improve Fourier transform artifacts. In this work, several window functions such as Hamming, Hanning, Blackman, Kaiser, and Tukey are used that implemented by Discrete Fourier Transform (DFT) in MATLAB code. Default window techniques in MATLAB were not used in these purposes. We applied window functions to the impulse response of those transmitted signals in Equations(12) and (18) to analysis which window technique gives better performance. The window function equations are [27]:

$$h(n)_{\text{hamming}} = 0.5\left[1 - \cos\left(\frac{2\pi n}{L-1}\right)\right]; 0 \le n \le \text{L} - 1, \tag{28}$$

$$h(n)_{\text{hanning}} = 0.54\text{-}0.46\cos\left(\frac{2\pi n}{L-1}\right)\Big]; 0 \le n \le L - 1, \tag{29}$$

$$h(n)_{\text{blackman}} = 0.42\text{-}0.5\cos\left(\frac{2\pi n}{L-1}\right)\Big] + 0.08\cos\left(\frac{4\pi n}{L-1}\right); \quad 0 \le \text{n} \le L - 1, \tag{30}$$

$$h(n)_{\text{kaiser}} = \frac{I_0\left[\alpha\sqrt{\left(\frac{L-1}{2}\right)^2 - \left(n - \frac{L-1}{2}\right)^2}\right]}{I_0\left[\alpha\left(\frac{L-1}{2}\right)\right]}, \tag{31}$$

$$h(n) = \begin{cases} 0.5\left\{1 + \cos\left(\frac{2\pi}{r}\left(n - \frac{r}{2}\right)\right)\right\}, 0 \le n < \frac{r}{2}, \\ 1, \frac{r}{2} \le x < 1 - \frac{r}{2}, \\ 0.5\left\{1 + \cos\left(\frac{2\pi}{r}\left(n - 1 + \frac{r}{2}\right)\right)\right\}, 1 - \frac{r}{2} \le n \le 1. \end{cases} \tag{32}$$

4. Result and Discussion

The section contains a description about the main findings of our works. It has been divided into three parts. The first step is to measure PAPR for fixed subcarriers at the transmitting end. Second, for 400 subcarriers, simulation results of conventional OFDM, FBMC, and UFMC with different modulation methods such as PSK and QAM are described. In our simulation, we use several channels: AWGN and Rayleigh Fading. After that, several window functions of filters were used. Finally, the simulated BER results were compared to the theoretical model. For simulation, MATLAB 2018b was used. Table 1 presents some of the most important simulation parameters in order to provide a clear picture of the simulated environment.

In Figure 4, for a specific point the PAPR value for classical model of OFDM, FBMC, and UFMC is 8.8856, 8.5673, and 8.6541 dB, respectively. From Figure 5, Hanning and

Table 1: Parameter definition chart.

Symbol parameters	OFDM	FBMC	UFMC
No. of subcarriers	600	600	600
No. of sub bands	×	×	40
Sub bands size	×	×	40
Overlapping factor	×	4	×
CP length	40	×	×
Channel	AWGN/Rayleigh/Rician	AWGN/Rayleigh/Rician	AWGN/Rayleigh/Rician
Modulation order	16 QAM/16 PSK	16 QAM/16 PSK	16 QAM/16 PSK

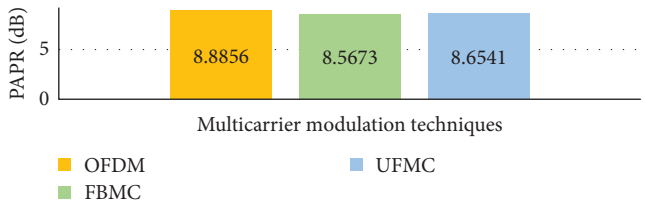

Figure 4: The PAPR values of traditional OFDM, FBMC, and UFMC system.

Tukey window techniques gave better result than traditional system in FBMC. Meanwhile, in UFMC, Kaiser and Tukey window techniques gave satisfactory output which was represented in Figure 6.

Figure 7 provided a comprehensive depiction of the performance evaluation of PAPR across multiple schemes. The proposed UFMC gave comparatively better performance in respect of PAPR. Correspondingly, Table 2 offered a succinct summary of the PAPR values which obtained from Figure 7. Specifically, at a designated point of 0.0001 on the *Y*-axis, the PAPR values stand at 12, 10, 8.5, and 7 dB for OFDM, FBMC, UFMC, and the proposed UFMC scheme, respectively. The proposed UFMC scheme exhibits superior PAPR performance compared to the conventional UFMC, FBMC, and OFDM. Table 2 revealed notable observations regarding the PAPR reduction achieved by the proposed scheme. A clear improvement was demonstrated by 5, 3, and 1.5 dB in comparison to the PAPR values of OFDM, FBMC, and UFMC, respectively. Our proposed method in UFMC outperformed OFDM and FBMC, exhibiting the lowest power levels in the top 10% of instances. For example, our proposed system gained almost 6% dB over the conventional system. The utilization of the Tukey window was associated with a remarkable decrease in BER accompanied by a low PAPR. This approach attained substantial BER reduction even under conditions of minimal SNR.

In Figure 8, the BER comparison was shown by using PSK modulation scheme in both simulation and theoretical perspective among OFDM, FBMC, and UFMC. For verify the simulated results with theoretical results, let us assume a SNR point 14 dB.

Table 3 demonstrates that the simulated and theoretical outcomes exhibited a high degree of similarity. However, the performance of BER fell short of expectations when employing PSK modulation. The simulated BER is 10^{-4} at near to 20 dB in UFMC and almost 10^{-4} at 20 dB in FBMC. But in OFDM, at 20 dB the BER was almost 10^{-3}, which is very poor compared to FBMC and UFMC.

Figure 9 displayed a comparative performance analysis of three conventional modulation techniques within the context of the AWGN channel. At SNR of 14 dB, both simulated and theoretically-derived results were tabulated for reference, as delineated in Table 4.

Table 4 revealed a notable alignment between the simulated and theoretical outcomes. However, it was imperative to underscore that the BER performance in PSK modulation fell short of the desired adequacy. The simulated BER is 10^{-4} at near to 20 dB in UFMC and almost 10^{-4} at 20 dB in FBMC. But in OFDM, at 20 dB the BER was almost 10^{-3}, which is very poor compared to FBMC and UFMC. In QAM, the BER was 10^{-5} at 14 dB in UFMC which is far better compared to FBMC and OFDM. From Figures 8 and 9, it became evident that there was a robust concurrence between the theoretical and simulated results. Moreover, it was noteworthy that QAM schemes exhibited superior performance in the context of UFMC compared to PSK schemes specifically within an AWGN channel.

Figures 10 and 11 illustrated the BER performance of OFDM, FBMC, and UFMC in a Rayleigh fading channel under different modulation schemes. It was observed that due to the presence of interference from additive noise, FBMC and UFMC exhibited poorer BER performance in the Rayleigh channel compared to the idealized AWGN channel. For example, in Figure 11, the QAM technique, at 14 dB, the BER of UFMC in Rayleigh fading channel was 1.25×10^{-2} whereas, in Figure 9, at AWGN channel, the BER is 10^{-4}. It's important to note that the power dissipation in a Rayleigh channel is significantly higher compared to an AWGN channel. This disparity in power dissipation could impact overall performance and may not consistently yield favorable results.

Figure 12 demonstrated that the Chebyshev filter outperforms the PHYDYAS filter in UFMC, delivering satisfactory performance while requiring lower power. Notably, at a random SNR point of 14 dB, the Chebyshev filter exhibited superior results.

The new filter approach in UFMC undergoes assessment even with higher order modulation schemes. Figure 13 illustrated the comparison of BER features between the proposed UFMC and the original UFMC signal across various QAM orders. Even with higher order modulations, the proposed UFMC consistently demonstrates superior BER performance.

Figure 14 depicted the BER performance of FBMC using different window techniques. To ascertain the most effective

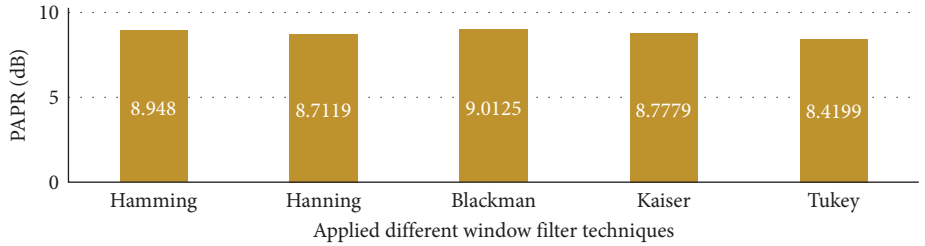

Figure 5: The PAPR values of FBMC by applying different window techniques.

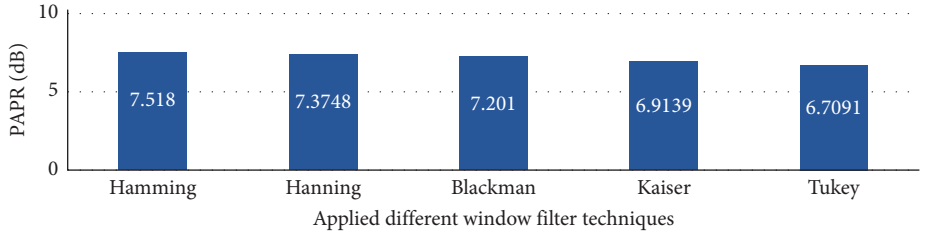

Figure 6: The PAPR values of UFMC by applying different window techniques.

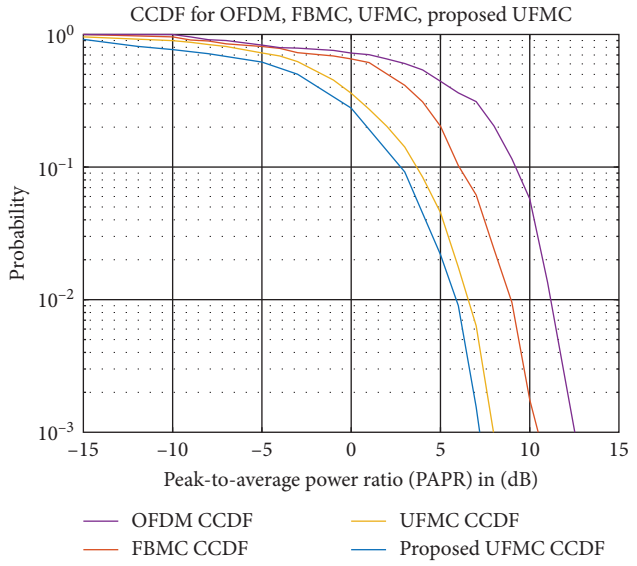

Figure 7: The CCDF of OFDM, FBMC, UFMC, and proposed UFMC system.

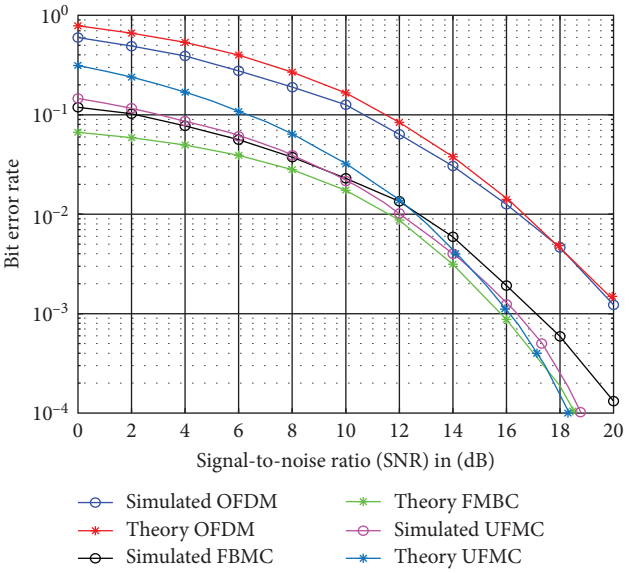

Figure 8: Conventional BER of OFDM, FBMC, and UFMC using PSK of AWGN.

Table 2: The value of CCDF of OFDM, FBMC, and UFMC at a fixed point.

MCM techniques	At 0.001
OFDM	12 dB
FBMC	10 dB
UFMC	8 dB
Proposed UFMC	7 dB

Table 3: Comparison between simulated and theoretical results in PSK.

MCM techniques	Simulated results	Theoretical results
OFDM	2×10^{-2}	3×10^{-2}
FBMC	5×10^{-3}	2×10^{-3}
UFMC	6×10^{-3}	3×10^{-3}

window technique, we evaluated BER at a random SNR of 14 dB, yielding varying BER values as outlined in Table 5. In Table 5, it was evident that the Kaiser window exhibited the most favorable BER response when compared to all other window techniques in aspect of power. This could be attributed to its effective suppression of stop-band ripples and the reduction of side-lobe bands, resulting in commendable performance within FBMC systems. But overall Tukey window gave best performance in aspect of SNR.

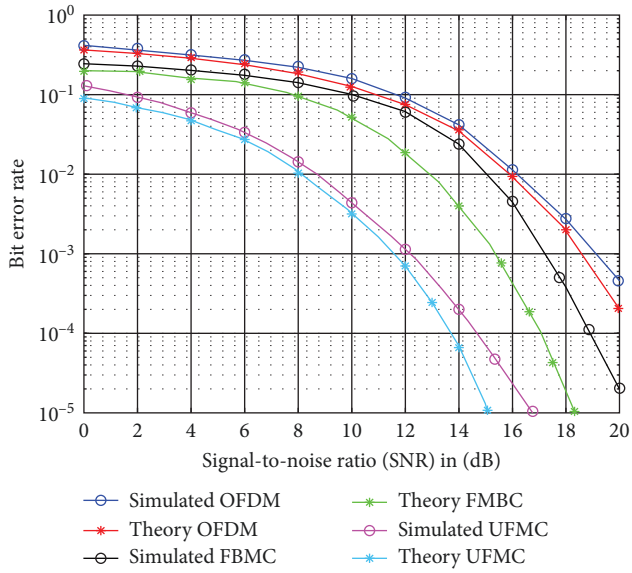

Figure 9: Conventional BER of OFDM, FBMC, and UFMC using QAM for AWGN.

Table 4: Comparison between simulated and theoretical results in QAM.

MCM techniques	Simulated results	Theoretical results
OFDM	1×10^{-2}	3×10^{-2}
FBMC	7×10^{-2}	1×10^{-2}
UFMC	10^{-5}	6×10^{-5}

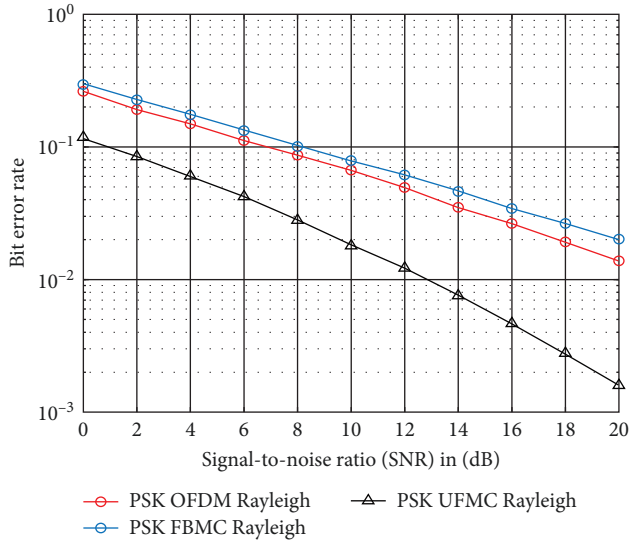

Figure 10: BER performance of OFDM, FBMC, and UFMC using PSK with 10 Tap Rayleigh channel.

Figure 15 illustrated the BER performance of UFMC employing various windowing functions. To determine the optimal BER performance among these windowing techniques, we considered a random SNR value of 14 dB. As detailed in Table 6, the Tukey window emerged as the top

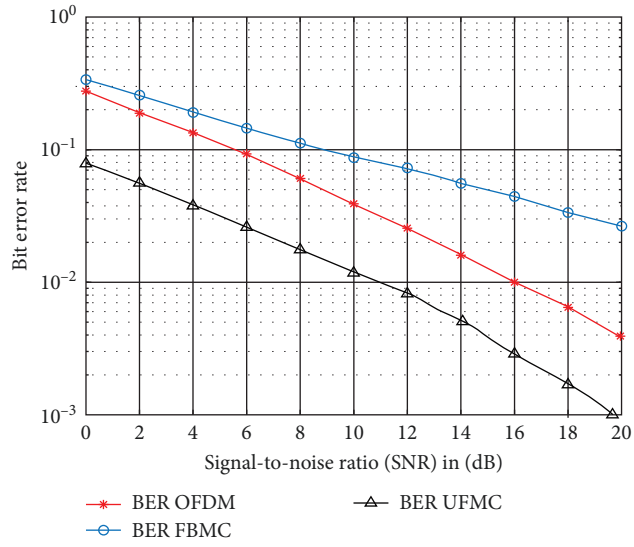

Figure 11: BER performance of OFDM, FBMC, and UFMC using QAM with 10 Tap Rayleigh channel.

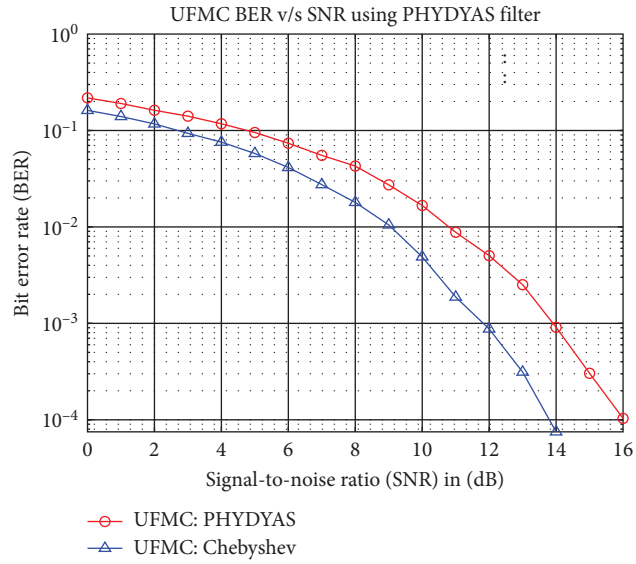

Figure 12: BER performance of UFMC using PHYDYAS and Chebyshev filter.

performer within the UFMC framework, especially at low SNR levels. This observation implied that the Tukey window demanded lower power consumption when compared to alternative filtering approaches.

In Figure 16, it was evident that, the performance of the Tukey window gave better performance than Chebyshev window through Rician Channel. In Table 7, a thorough comparison between the Chebyshev and Tukey windows revealed a distinct advantage for the Tukey window, demonstrating a 24% enhancement in output performance. Consequently, employing the Tukey window not only yields superior results but also consumes less power, underscoring its efficacy in achieving optimized outcomes.

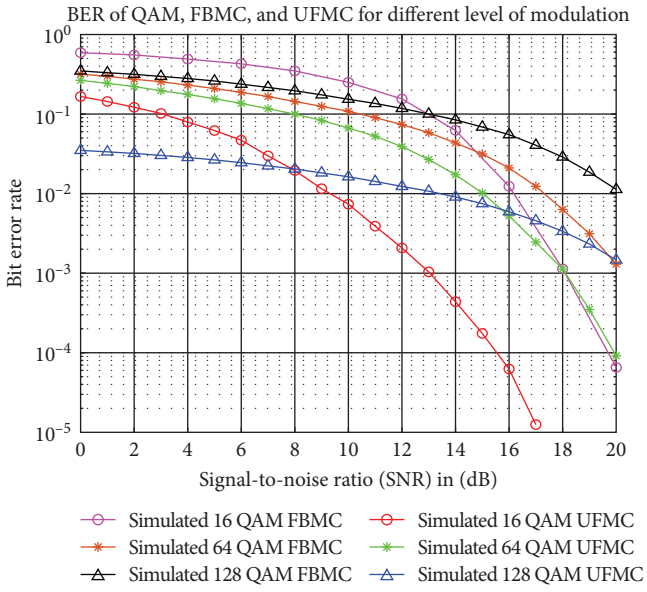

Figure 13: BER performance of UFMC using different level of QAM.

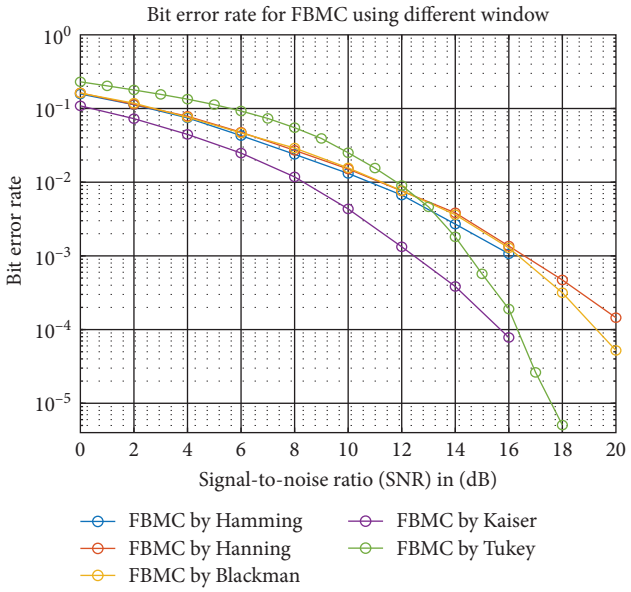

Figure 14: BER performance of FBMC using different windows.

Table 5: BER values of different windows in FBMC.

Window functions	Bit error rate
Hamming	1.9×10^{-3}
Hanning	3×10^{-3}
Blackman	3×10^{-3}
Kaiser	3×10^{-4}
Tukey	1×10^{-3}

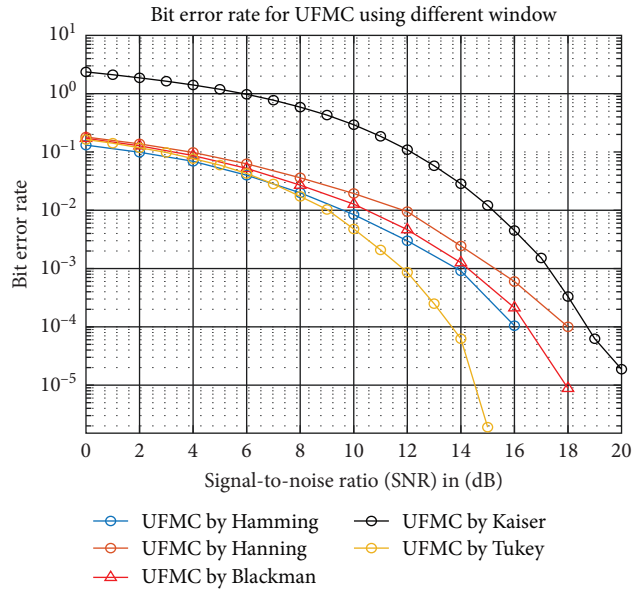

Figure 15: BER performance of UFMC using different windows through AWGN channel.

Table 6: BER values of different windows in UFMC.

Window functions	Bit error rate
Hamming	10^{-3}
Hanning	2×10^{-3}
Blackman	10^{-3}
Kaiser	2×10^{-3}
Tukey	6×10^{-5}

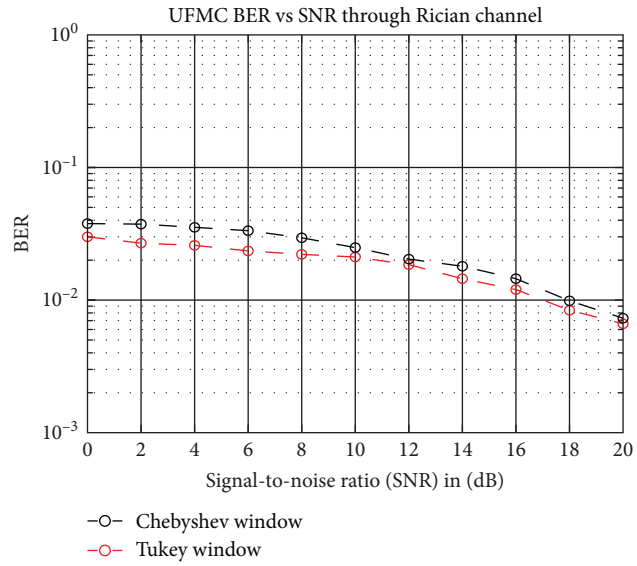

Figure 16: BER performance of UFMC using Chebyshev and Tukey filter through Rician channel (K-factor = 3).

Table 7: BER values of UFMC through Rician channel.

Modulation technique	Window	Bit error rate
UFMC	Chebyshev	1.8×10^{-2}
	Tukey	1.45×10^{-2}

Table 8: Comparison between existing system and proposed system.

Modulation scheme	Existing system	Proposed system
FBMC	$10^{-3.7}$ [28]	10^{-4}
	1.58×10^{-3} [29]	
UFMC	4×10^{-2} [30]	$\sim 10^{-6}$
	5.7×10^{-2} [29]	

In the context of our research study, which involved the application of diverse filtering techniques, UFMC with a Tukey filter was less prone to errors compared to other systems in terms of PAPR and BER across both FBMC and UFMC systems.

The Blackman window incorporated an additional cosine term which helps reduce side lobes, especially when compared to the Hamming and Hanning windows, leading to improved BER performance. For applications where superior stop-band attenuation was required, the Kaiser window outperformed the Blackman window. This was particularly advantageous in FBMC systems, where minimizing signal leakage between sub bands is crucial. Nevertheless, the Tukey window offered even more effective stop band reduction. In combination with a 2N point FFT and ZP, it could significantly enhance BER and PAPR performance in UFMC systems. This combination of factors made the Tukey window an excellent choice for applications demanding stringent stop band control and spectral containment.

The BER of FBMC–OQAM scheme was nearly $10^{-3.7}$ at 18 dB [28] and 1.58×10^{-3} at 20 dB [29]. We found 10^{-4} at 16 dB in Kaiser window in FBMC shown in Figure 15. The BER of UFMC was zero at 25 dB at [30]. The outcome of BER, using of the significant inter-service-band-interference (ISBI) cancellation algorithm, is yielded a value of 5×10^{-3} at 30 dB [31]. The BER of UFMC using resource block (RB) system is 10^{-3} [32]. In UFMC, we identified zero at 15 dB using the Tukey window filter (Figure 15). However, it's important to note that the Tukey window had limitations in reducing side lobe bands compared to the Blackman window, due to the absence of an additional cosine term. This could result in higher noise response with the Blackman window. The new filtering method in UFMC demonstrated a significant improvement over OFDM, reducing bit errors by 81%, with a difference of 0.01994. Meanwhile, the new filtering technique approach showed a substantial enhancement compared to conventional UFMC and FBMC, achieving a remarkable 91% reduction in bit errors, with a margin of 0.06994 as the key distinction. Under the premise of meeting ideal reconstruction conditions, it could be inferred that the performance of AWGN and Rayleigh channel methods might be same aspect of OFDM and FBMC [33]. The UFMC technique demonstrated an energy advantage over OFDM when subjected to minor frequency shifts within the AWGN channel [34]. The effects of timing offset (TO), CFO, and phase noise on the performance of OFDM were unfavorable in terms of BER [35]. Furthermore, in terms of CCDF, the average power registers at 9.5 dB for 16 QAM. However, within our system, the power level stands at 7 dB for 16 QAM, indicating a notable reduction of 30% in power loss [36].

A comprehensive analysis of the UFMC system, a simpler methodology incorporating filtering techniques, had been introduced. The obtained results using Tukey window filter clarified the achievable data rate of the proposed scheme which is shown in Table 8. Simulation outcomes demonstrated the efficacy of the new filtering techniques in UFMC-based approaches in effectively mitigating interference, thereby yielding improved performance in terms of PAPR and BER compared to DC and PHYDYAS filter using in UFMC. Overall, when considering all results, UFMC with Tukey window emerged as one of the most effective candidates for 5G technology in the current landscape.

5. Conclusion

This study introduces a new filtering technique aimed at enhancing the efficiency of FBMC and UFMC systems. The simulation outcomes indicate that UFMC exhibits superior characteristics when compared to both FBMC and OFDM.

Simulation results indicate that the proposed UFMC system surpasses conventional UFMC, FBMC, and OFDM systems in terms of SNR and CCDF outcomes. The results of simulations assessing BER performance within realistic channel models demonstrate that the suggested filter implementation in FBMC and UFMC systems outperforms conventional systems.

The main challenge of UFMC high computational complexity for transceivers is tackled in this paper by using different mapping, channels, and filter techniques. Furthermore, the proposed system utilizes consistent precoding to diminish PAPR, enhancing robustness without the need for additional power increments or intricate optimizations compared to conventional systems. In addition, it is worth mentioning that the proposed UFMC transceivers have the lowest computational complexity among the 5G candidates FBMC, f-OFDM.

Our proposed system is suitable for future use in implementing 3GPP-compliant new waveforms within OpenAir Interface. Subsequent efforts will focus on the hardware implementation of the proposed system to ascertain the postsynthesis hardware complexity.

Data Availability

All data are generated and simulated using the Matlab software tool. Authors are able to provide all the source codes.

Conflicts of Interest

The author(s) declare(s) that there is no conflict of interest regarding the publication of this paper.

Acknowledgments

This study was funded in a self-financing way.

References

[1] S. Wei, H. Li, W. Zhang, and W. Cheng, "A comprehensive performance evaluation of universal filtered multi-carrier technique," *IEEE Access*, vol. 7, pp. 81429–81440, 2019.

[2] Y. Medjahdi, S. Traverso, R. Gerzaguet et al., "On the road to 5G: comparative study of physical layer in MTC context," *IEEE Access*, vol. 5, pp. 26556–26581, 2017.

[3] K. Zerhouni, F. Elbahhar, R. Elassali, and K. Elbaamrani, "Performance of universal filtered multicarrier channel estimation with different pilots arrangements," in *2018 IEEE 5G World Forum (5GWF)*, pp. 327–332, IEEE, Silicon Valley, CA, USA, 2018.

[4] H. M. Abdel-Atty, W. A. Raslan, and A. T. Khalil, "Evaluation and analysis of FBMC/OQAM systems based on pulse shaping filters," *IEEE Access*, vol. 8, pp. 55750–55772, 2020.

[5] B. Farhang-Boroujeny, *OFDM Versus Filter Bank Multicarrier*, vol. 28, pp. 92–112no. 3, IEEE Signal Processing Magazine, 2011.

[6] C. Kim, Y. H. Yun, K. Kim, and J.-Y. Seol, "Introduction to QAM-FBMC: from waveform optimization to system design," *IEEE Communications Magazine*, vol. 54, no. 11, pp. 66–73, 2016.

[7] A. Sahin, I. Guvenc, and H. Arslan, "A comparative study of FBMC prototype filters in doubly dispersive channels," in *2021 IEEE Globecom Workshops*, pp. 197–203, IEEE, 2012.

[8] L. Sakkas, E. Stergiou, G. Tsoumanis, and C. T. Angelis, "5G UFMC scheme performance with different numerologies," *Electronics*, vol. 10, no. 16, Article ID 1915, 2021.

[9] A. K. M. Baki, R. A. Ahsan, and A. Awsaf, "Novel methods of filtering for FBMC/UFMC based 5G communication systems," in *2019 7th International Conference on Smart Computing & Communications (ICSCC)*, pp. 1–4, IEEE, 2019.

[10] Z. Guo, Q. Liu, W. Zhang, and S. Wang, "Low complexity implementation of universal filtered multi-carrier transmitter," *IEEE Access*, vol. 8, pp. 24799–24807, 2020.

[11] G. A. Hussain and L. Audah, "BCH codes in UFMC: a new contender candidate for 5G communication systems," *Bulletin of Electrical Engineering and Informatics*, vol. 10, no. 2, pp. 904–910, 2021.

[12] R. S. Yarrabothu and U. R. Nelakuditi, "Optimization of out-of-band emission using kaiser-bessel filter for UFMC in 5G cellular communications," *China Communications*, vol. 16, no. 8, pp. 15–23, 2019.

[13] S. Dhua, R. Arjun, K. Appaiah, and V. M. Gadre, "Low complexity FBMC with filtered OFDM for 5G wireless systems," in *2020 International Conference on Signal Processing and Communications (SPCOM)*, IEEE, 2020.

[14] A. A. Molla, M. F. Ahammed, and M. I. Kadir, "Evaluation of UFMC as a potential waveform contender of OFDM for next-generation wireless," in *2021 International Conference on Electronics, Communications and Information Technology (ICECIT)*, IEEE, 2021.

[15] S. Ramavath, P. K. Patra, and U. C. Samal, "Theoretical analysis of power spectral density of CP-based FBMC signals," in *2023 International Conference on Communication, Circuits, and Systems (IC3S)*, IEEE, 2023.

[16] D. Khosla and S. Singh, "OFDM modulation technique & its applications: a review," in *International Conference on Innovations in Computing (ICIC 2017)*, pp. 101–105.

[17] T. Jiang, D. Chen, C. Ni, and D. Qu, *OQAM/FBMC for Future Wireless Communications: Principles, Technologies and Applications*, Academic Press, 2017.

[18] Y. S. Cho, J. Kim, W. Y. Yang, and C. G. Kang, *MIMO-OFDM Wireless Communications with MATLAB*, John Wiley & Sons, 2010.

[19] T. Jiang, D. Chen, C. Ni, and D. Qu, "Power spectral density of OQAM/FBMC," in *OQAM/FBMC for Future Wireless Communications*, pp. 39–68, Elsevier, 2018.

[20] S. S. Alam and A. Saha, "Performance analysis of FBMC over OFDM for high data rate MIMO configurations," *International Journal of Wireless and Microwave Technologies*, vol. 11, no. 4, pp. 20–33, 2021.

[21] F. S. Hasan and N. Q. Lateef, "Performance comparison of multicarrier communication systems over doubly-selective channels," *Periodicals of Engineering and Natural Sciences*, vol. 9, no. 3, pp. 12–21, 2021.

[22] L. Yao, E. Wang, and X. Peng, "Design and research on FBMC-OQAM multicarrier technology for 5G," in *Journal of Physics: Conference Series*, IOP Publishing, Article ID 052068.

[23] M. Wu, J. Dang, Z. Zhang, and L. Wu, "An advanced receiver for universal filtered multicarrier," *IEEE Transactions on Vehicular Technology*, vol. 67, no. 8, pp. 7779–7783, 2018.

[24] P. N. Rani and C. S. Rani, "UFMC: The 5G modulation technique," in *IEEE International Conference on Computational Intelligence and Computing Research (ICCIC)*, pp. 1–3, IEEE, 2016.

[25] S. Sidiq, F. Mustafa, J. A. Sheikh, and B. A. Malik, "FBMC and UFMC: the modulation techniques for 5G," in *2019 International Conference on Power Electronics, Control and Automation (ICPECA)*, pp. 1–5, IEEE, 2019.

[26] D. E. Kebiche, A. Baghaki, X. Zhu, and B. Champagne, "UFMC-based wideband spectrum sensing for cognitive radio systems in non-Gaussian noise," in *IEEE 28th Annual International Symposium on Personal, Indoor, and Mobile Radio Communications (PIMRC)*, pp. 1–7, IEEE.

[27] J. G. Proakis, *Digital Signal Processing: Principles Algorithms and Applications*, Pearson Education India, 2001.

[28] M. A. Taher and K. H. Kutheir, "FBMC as 5G candidate for high-speed mobility," *IOP Conference Series: Materials Science and Engineering*, vol. 557, no. 1, Article ID 012040, 2019.

[29] H. T. Dumari, D. J. Gelmecha, R. K. Shakya, and R. S. Singh, "BER and PSD improvement of FBMC with higher order QAM using Hermite filter for 5G wireless communication and beyond," *Journal of Electrical and Computer Engineering*, vol. 2023, Article ID 7232488, 16 pages, 2023.

[30] R. T. Kamurthi, S. R. Chopra, and A. Gupta, "Higher order QAM schemes in 5G UFMC system," in *International Conference on Emerging Smart Computing and Informatics (ESCI)*, pp. 198–202 (2020), 2020.

[31] L. Zhang, A. Ijaz, P. Xiao, A. Quddus, and R. Tafazolli, "Subband filtered multi-carrier systems for multi-service wireless communications," *IEEE Transactions on Wireless Communications*, vol. 16, no. 3, pp. 1893–1907, 2017.

[32] H. Kim, J. Bang, S. Choi, and D. Hong, "Resource block management for uplink UFMC systems," in *2016 IEEE Wireless Communications and Networking Conference*, pp. 1–4, IEEE, 2016.

[33] Q. He and A. Schmeink, "Comparison and evaluation between FBMC and OFDM systems," in *WSA 2015 19th International ITG Workshop on Smart Antennas*, pp. 1–7, 2015.

[34] G. Bochechka, V. Tikhvinskiy, I. Vorozhishchev, A. Aitmagambetov, and B. Nurgozhin, "Comparative analysis of UFMC technology in 5G networks," in *International Siberian Conference on Control and Communications (SIBCON)*, pp. 1–6, IEEE, 2017.

[35] B. Lim and Y.-C. Ko, "SIR analysis of OFDM and GFDM waveforms with timing offset, CFO, and phase noise," *IEEE Transactions on Wireless Communications*, vol. 16, no. 10, pp. 6979–6990, 2017.

[36] K. K. Kishore, P. R. Umar, and V. J. Naveen, "Comprehensive Analysis of UFMC with OFDM and FBMC," *Indian Journal of Science and Technology*, vol. 10, no. 17, pp. 1–7, 2017.